Time-dependent behaviour of hard rock in deep level gold mines

by D.F. Malan*, U.W. Vogler*, and K. Drescher*

Synopsis

In deep level hard rock mining the rheological behaviour of the rock is important as time-dependent aseismic processes can lead to a stable dissipation of energy thus reducing violent outbursts. Underground closure measurements, observations of time-dependent fracture formation and siesmic data indicate that the rock in deep South African gold mines shows significant time-dependent behaviour. The objective of this work is to quantify the time-dependent rock behaviour for laboratory specimens and underground conditions. Laboratory experiments indicated that lava and quartzite specimens undergo measurable creep strain at stress magnitudes below the failure stress. Quartzite is however prone to more significant creep at lower stress levels. A viscoelastic analysis showed that laboratory creep results can not fully explain the behaviour observed underground. The *in situ* behaviour is governed mainly by the rheological behaviour of the fracture zone and the resulting time-dependent formation of new fractures. A viscoplastic discontinuity model implemented in a boundary element program is used to simulate this behaviour.

Introduction

Knowledge of rock deformation and yield surrounding deep level openings in hard rock is of significant interest to engineers in the South African mining industry. Although important progress was made in research of this topic over past decades, a complete understanding of the fracture zone development surrounding these excavations has not yet been achieved. Commonly, elastic and elastoplastic constitutive models are used to determine stresses and strains around openings. A disadvantage of these models is that the time factor is ignored.

As the term creep is commonly used to describe different types of time-dependent rock behaviour, the following definitions are introduced to avoid confusion. *Creep* is continued deformation due to a constant applied stress and will be used exclusively in relation to laboratory-sized specimens containing no large- scale discontinuities. *Time-dependency* is a more general term encompassing concept like creep, rate-dependent behaviour, delayed fracturing and long-term strength. As the rheological behaviour of the rockmass underground is a complex interrelation of these factors, it will therefore be referred to as *time-dependency*. When used in relation to underground measurements, time dependency is also understood to refer to deformations not related to geometric changes in the dimensions of an excavation. It occurs on a time scale of days to years and is therefore not related to elastodynamic behaviour.

Creep of rocks has been studied since the early part of this century (Griggs[1]) resulting in the availability of a vast amount of data. Most of the studies however focused on the softer saltrocks because they show significant creep under stress and temperature conditions easily applied in the laboratory. (See Lama and Vutukuri[2] and Dusseault and Fordham[3] for a detailed summary of creep studies.) This paper will focus on the time-dependent behaviour of hard rocks found in South African gold mines. Results of the laboratory creep of quartzite and lava specimens will be presented. This will be contrasted with time-dependent behaviour measured underground.

The need for research into time-dependent rock behaviour

Researchers (Roux and Denkhaus[4]; Denkhaus *et al*.[5]) recognised as early as the fifties that the time-dependent behaviour of rock is important as it may cast light on why rockbursts do not always occur at blasting time but also when there is no external influence which could account for changes in stress distribution. Significant time-dependent deformation may also cause a gradual non-violent release of abutment

* *CSIR Division of Mining Technology, P.O. Box 91230, Auckland Park, 2006.*

 SA ISSN 0038–223X/3.00 + 0.00. Paper received Dec. 1996; revised paper received Apr. 1997.

stress and hence diminish the danger of rockbursts. Although not directly related to hard rock, Pomeroy[6] carried out creep experiments on a number of coal specimens. Anthracite samples did not creep (within the limits of sensitivity of the equipment used) and always failed explosively. He related this to the frequent occurrence of violent outbursts in anthracite mines. These outbursts are much less common in mines where significant creep is observed in the coal. Similarly, Denkhaus *et al*.[5] noted that the susceptibility to bursts was much more prevalent in stopes in the Central Rand, where the reef lies between hard brittle quartzite bands, than on the Far East Rand where the reef lies on ductile shale.

One strategy which may be useful in controlling the stability of the fracture zone is the rate of stope face advance. An appropriate time-dependent constitutive law could lead to some generalisations regarding safe values of extraction rate and better control of the fracture zone. Research is being directed towards finding this appropriate constitutive description of hard rock in the South African mining industry.

Time-dependent rock behaviour plays a further important role in determining the long-term stability of service excavations and the behaviour of pillars where delayed fracture may lead to eventual failure. Potts and Hedly[7] pointed out that:

'One of the most important features of a material which exhibits "creep" characteristics is the incidence of delayed fracture. In mining this would imply that a room-and-pillar area, which is stable immediately after extraction deteriorates in time and ultimately goes to failure'.

Laboratory testing of creep in South African hard rocks

In an attempt to quantify these effects in the South African industry, some initial studies on the time-dependent behaviour of hard rock were conducted in the sixties by the Rock Mechanics Division of the CSIR's National Mechanical Engineering Research Institute (Wiid[8]; Kovács[9]). These studies concentrated on the creep of intact specimens and on long-term strength measurements. Unfortunately a systematic study of the creep of hard rock throughout the industry was never conducted, probably due to the long duration of individual tests and the lack of funding. The situation was further aggravated by a school of thought which associated creep phenomena exclusively with soft rocks like halite and potash. The need for the time-dependent testing of hard rock, whether for intact samples, discontinuities or *in situ*, has not always been recognised.

The following laboratory work on the time-dependent behaviour of South African hard rocks was nevertheless conducted. Roux and Denkhaus[4] published results for the creep of quartzite at room temperature as shown in Figure 1. Unfortunately no information on the type of quartzite or test methodology is available. However, what is significant is that measurable creep was observed for the quartzite specimen. Typical primary and secondary creep phases can be distinguished from Figure 1 with the primary phase lasting approximately 2 days (See Lama and Vutukuri[2] for a definition of primary, secondary and tertiary creep). The creep strain rate in the secondary phase for the applied stress of 32.9 MPa was calculated as 2.6×10^{-11} s^{-1}.

The CSIR[10] conducted further experiments on quartzites from the Hartebeestfontein mine. The quartzite specimens were medium-grained argillaceous samples obtained from a single borehole. The rock properties, however, varied considerably along the length of the borehole due to alternating argillaceous and siliceous bands in some sections. The uniaxial compressive strength for different samples varied between 117 MPa and 248 MPa with an average 192 MPa. Specimens were subjected to a constant uniaxial compressive stress of 138 MPa in a deadweight testing machine. Examples of the strain-time curves obtained are displayed in Figure 2. It is immediately evident that the creep behaviour also showed appreciable differences between different samples. Unfortunately no attempt was made to analyse this behaviour quantitatively or to link it to the geology of individual specimens. The creep rate in the secondary phase (calculated from Figure 2) varied between 1.6×10^{-8} s^{-1} and 1×10^{-9} s^{-1}. These values should however be considered as approximate only as it is difficult to determine the onset of the secondary creep phase.

Further studies concentrated mainly on the long-term strength of rock. Bieniawski[11] showed that the long-term strength of rock under uniaxial loading can be determined from the plot of axial stress versus

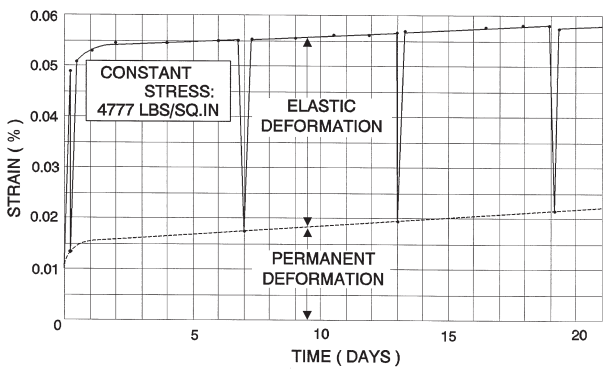

Figure 1—Creep curve for quartzite at room temperature (After Roux and Denkhaus[4]). The applied stress is 32.9 MPa in metric units

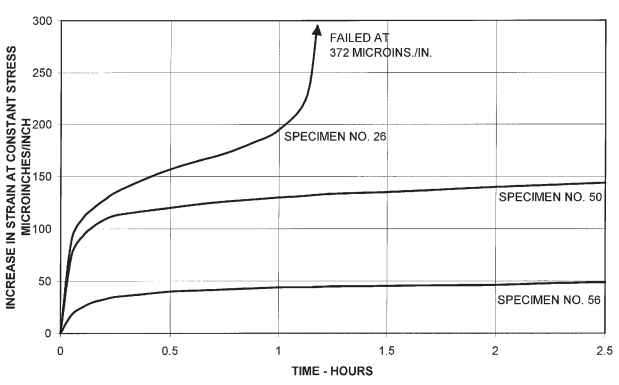

Figure 2—Creep curves obtained for quartzite from Hartebeestfontein Goldmine (after CSIR[10]). The applied stress was 138 MPa

volumetric strain. The onset of unstable fracture propagation (the point on the plot where the slope changes from negative to positive) indicates the long-term strength. Tests on norite samples showed that the long-term strength can be as low as 73% of the uniaxial compressive strength. Bieniawski's hypothesis was confirmed by experiments conducted by Wiid[8] on dolerite and sandstone. Again, the long-term strength could be as low as 70% of the uniaxial compressive strength. Kovács[9] investigated the relationship between time to failure (t_F) and applied load (σ_t) for samples of quartzite with $\sigma_L < \sigma_t < \sigma_C$ where σ_L is the long-term strength and σ_C the uniaxial compressive strength. The following empirical relationship was used to represent this relationship.

$$t_F = a\left(\frac{1}{i} \pm 1\right)^b \qquad [1]$$

where

$$i = \frac{\sigma_t \pm \sigma_L}{\sigma_C \pm \sigma_L}. \qquad [2]$$

For argillaceous quartzite, the calculated values of a and b were 24.75 and 1.95 respectively (for t_F calibrated in hours).

In situ *measurements of time-dependent rock behaviour*

Apart from the laboratory experiments, significant time-dependent rock behaviour was noted by reseachers monitoring stope closure behaviour underground. King *et al.*[12] measured closure behaviour in two adjacent panels at Hartebeesfontein Gold Mine. After blasting activity had been stopped in one of the panels, the closure rate in this panel continued at a constant rate of 6mm/day for 37 days. Only after this period did the rate gradually start to decrease. Mining however continued in the second panel (and probably in other nearby panels) and it is unclear what the effect of these geometrical changes were on the first panel. After mining stopped in the second panel the closure rate in this panel persisted for 13 days and then gradually declined. Closure data collected by Gürtunca[13] in the Klerksdorp area to quantify the effect of backfill also exhibited significant time-dependent effects. Daily closure rates varied from panel to panel and were in some instances as high as 30 mm/day. The study showed that closure rates are significantly lower in backfilled panels than in partially filled panels.

The true time-dependent behaviour of the rock mass is difficult to identify from daily measurements as the data also contains the effect of changes in the mining geometry. This problem can be overcome partially by taking closure measurements with instruments which record in a continuous fashion. From this the time-dependent closure behaviour between successive blasts (when there is no change in mining geometry) can be identified.

The following observations and analysis of continuous closure measurements are described in literature. Leeman[14] used closure recorders to measure continuous closure profiles in a tabular stope at East Rand Proprietary Mines.

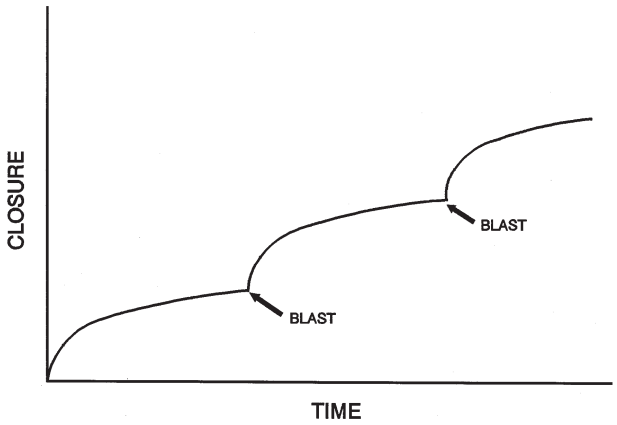

Figure 3—Typical profile of stope closure as a function of time

For a typical stope the rate of closure suddenly increased just after blasting time. This high rate of closure decreased within hours to give a gradual steady-state closure until the next blast occured and the pattern repeated (Figure 3). Leeman did not give any explanation for the observed closure profiles although he did note that the amount of closure caused by blasting diminished with increasing distance from the working face. The rate of closure also varied greatly from one point to the next and was affected by the position of the measuring point in relation to the support in the stope. What is significant about these measurements is that the time-dependent closure is much larger than can be accounted for by the creep of intact rock material alone. Movements in the order of millimeters can be observed in a matter of hours.

Hodgson[15] also measured continuous closure in East Rand Proprietary Mines. He explained time-dependent closure as being caused by the time-dependent migration of the fracture zone ahead of the face resulting in the effective span becoming bigger. Hodgson predicted that if the face advanced faster than the migration of the fracture zone, less energy would be released in a stable manner thereby increasing the incidence of rockbursts. This is in agreement with the statistical analysis of Cook *et al.*[16] which indicated an increase in rockbursts for a face advance rate of more than 4 metres a month for small abutments to 8 metres a month for large abutments.

Experimental evidence of time-dependent fracture formation was obtained by Adams and Jager[17] who investigated the extent of the fracture zone that occurs ahead of advancing stope faces at the Doornfontein gold mine. They found the formation of fractures to be associated with face advance, where the majority of new fractures form within a relatively short period after blasting. The amount of new fracturing taking place then diminishes as the face stands. No new fractures could be observed for faces that were not mined for a period of 14 days.

The first quantitative attempt to analyse continuous closure profiles of tabular stopes was made by McGarr[18] using data from East Rand Proprietary Mines. He used an empirical approach to represent the closure δ as

$$\delta = \frac{B}{C} \sum_{n=0,1,\ldots,n\neq m,m=1,2,\ldots}^{\infty} \left(1 \pm e^{\pm DC(t \pm 24n)}\right) H(t \pm 24n) \qquad [3]$$

where *B*, *C* and *D* are positive constants, *n* and *m* are integers representing number of days and H is the Heaviside unit function (H(t) =1 for t ≥ 0 and 0 for t <0). The unit of time t in the equation is hours. At the time of this study no blasting on Sundays was allowed and n = 7m corresponds to those days. Obtaining the rate of closure from equation [3] by differentiating gives

$$\dot{\delta} = DB \sum_{n=0,1,\ldots,n\neq 7m,m=1,2,\ldots.}^{\infty} e^{\pm DC(t\pm 24n)} H(t \pm 24n) \qquad [4]$$

After the last blasting period of the week on Saturday, the closure and the rate of closure become

$$\delta = a\left(1 \pm e^{\pm\frac{t}{\tau}}\right) \qquad [5]$$

and

$$\dot{\delta} = be^{\pm\frac{t}{\tau}} \qquad [6]$$

respectively where a and b are constants and $\tau=1/DC$. McGarr[18] suggested the relaxation time τ may be used as a parameter to describe the ability of the rock mass to form a fracture zone in response to face advance. High values of τ might be associated with mines that are prone to rockbursts.

Malan[19] used a viscoelastic approach to model continuous closure profiles of tabular excavations after blasting. An analytical solution for the time-dependent closure behaviour of a parallel-sided panel without total closure in the back area was derived. A good fit was obtained between the model and experimental closure data. The limitation of the model however is that it assumes the rock mass to be a continuum viscoelastic material and is therefore unable to simulate the fracture process in the immediate area of the stope.

Seismicity and time-dependent rock behaviour

Further evidence of time-dependent processes in rock was obtained from seismic data. For the typical daily distribution of seismicity, Cook[20] found that the incidence of events is greatest during and immediately after blasting. A large proportion of the events nevertheless occurs throughout the remainder of the day as does much of the total amount of energy released. This evidence indicates that the rock failure process must be time-dependent in nature. McGarr[21] investigated the dependence of magnitude statistics on aseismic rock deformation in the East Rand Proprietary Mines. There appeared to be a strong correlation between the level of seismicity and the rate of aseismic deformation. That is, the time-dependence of the seismicity is the result of aseismic deformation that occurs over an extended period. It appeared that the rock was undergoing logarithmic creep in response to stress changes due to either mine face advance or to seismic events. It was postulated that the aseismic deformation was due to progressive brittle failure as the rock temperature was too low to allow for continuum plastic deformation in the quartizites.

Stewart and Spottiswoode[22] discussed cumulative seismicity with time after blasting for data obtained from an experimental preconditioning site at Blyvooruitzicht Gold Mine. The data exhibits three clear trends, namely an initial steep linear portion corresponding to the blast sequence itself, an intermediate portion in which the cumulative seismicity rate is inversely proportional to time, and a final portion which corresponds to the background level of seismicity. The data set was, however, limited to the first hour after blasting.

Van Aswegen and Butler[23] monitored time-dependent movement of a major fault in the Welkom goldfields. An average displacement rate of 1 mm/month was recorded on the fault. The cumulative apparent volume (see reference[24] for a definition) of seismic events in the rock surrounding the fault showed significant correlation with the measured movement.

Time-dependent rock behaviour has been noted by Mendecki[25] through his involvement in developing real time quantitative seismic systems for the mining industry. Concepts like seismic viscosity and seismic relaxation time have been used to quantify rheological characteristics of the rock mass[24]. It has been noted that a decrease in seismic viscosity with time is frequently observed at some stage before rock instability.

From the various studies described above, it is clear that there is only a limited understanding of the time-dependent behaviour of South African hard rocks in the deep level gold mines. There is virtually no data available on the laboratory creep of these rocks. Results of the creep of a typical quartzite and lava specimen as determined in the laboratory will be presented in this paper. The test methodology is described in the next section.

Table I

	Quartzite	Lava
Test specimen number	1355-CRP-05	1640-CRP-63
Rock type	Argillaceous footwall quartzite (Lorraine)	Ventersdorp lava (Western Deep Levels)
Starting date of test	1989-09-21	1995-10-28
Duration of creep stages	24 hours	72 hours
Total number of full creep stages	23	4
Testing machine	Amsler	CSIR creep tester
Method of maintaining constant load	Servo-control	Deadweights
Partial unloading before next stage	No	Yes
Density	2170 kg/m^3	2920 kg/m^3
Failure stress	116 MPa	402 MPa
Young's modulus	66 GPa	92 GPa
Failure during load increase	Yes	No
Failure within minutes of load increase	No	Yes
Control specimen properties		
Uniaxial compressive strength	38 MPa	430 MPa
Young's modulus	59 MPa	95 MPa

Laboratory testing methodology

Load application principles

Laboratory creep tests on the quartzite and the lava specimens were performed as part of other investigations using different testing equipment. Full details of the tests have been reported by Vogler[26] and Vogler and Drescher[27]. The data has however never been analysed. The similarities and the differences in the testing methodology are summarised in Table I.

Two methods of conducting laboratory creep experiments are available namely:

- Specimens are loaded to a pre-determined, constant stress level. This stress level may, for instance, be the stress level expected around a mining excavation. The creep strain and the time to failure may be monitored. If, however, the aim of the testing programme is to fully characterise the creep behaviour of the material or its time-dependent strength characteristics, many tests have to be performed at different stress levels. If the material properties vary considerably it may be difficult to determine the time-dependent strength (the time to failure for the material when loaded to a particular stress) or the long-term strength (the stress below which failure will not occur). It may happen that a specimen loaded to a certain stress level fails after a few days while another loaded to the same stress level does not fail after a period of months. This could be the result of a stress level chosen which is just above or below the specimen's long-term strength.
- The same specimen is loaded to different stress levels by starting at a low value and increasing the stress in steps after allowing a certain time interval for creep. The obvious advantage of this approach is that the creep strain may be monitored for an 'identical' material at different stress levels and that each specimen will be tested to failure within a reasonable time. The total test duration is determined by the choice of the stress level of the first creep stage, the duration of each creep stage and the magnitude of subsequent stress level increases. A similar methodology was used by Tan[28].

This second approach was used for the tests described in this paper. When performing long duration tests requiring attention at regular intervals, it is advisable to use 24-hour creep cycles or multiples thereof. For the test on the quartzite, the duration of the creep stages was 24 hours and for the lava, 72 hours.

Testing equipment

For the tests on the quartzite, a servo-controlled Amsler compression testing machine was used. Minor fluctuations in load (below 0.1 MPa) took place as the machine continuously made the necessary adjustments. Loading to each successive stress level was achieved by adjusting the settings of the load control.

For the tests on the lava the CSIR creep testing machine, described by Bieniawski[11], was used. This machine makes use of deadweights and cantilevers to maintain the desired load. Loading to the next stress level was done by adding further weights. For this test, each loading step was preceded by a partial unloading step to monitor any change in deformation modulus during loading and unloading.

Strain measurements

Strain measurements were obtained by using strain gauges and inductive transducers. The inductive transducer measurements were used to monitor any possible creep in the strain gauges. No noticeable creep was observed and the strain gauge measurements, giving higher resolution, were used for subsequent evaluations.

Due to the minor fluctuations in the load applied to the quartzites by the compression testing machine, the strain values measured for the creep period were corrected to a constant stress level by using the elastic modulus for the specimen as determined from the initial loading cycle.

Temperature

The laboratory experiments were performed at room temperature. The Amsler machine is housed in an open laboratory, subject to ambient temperature variations. This was in turn influenced by the heat generated by the machine. Therefore the temperature of the test specimen was monitored throughout the experiment. For the quartzite, the experiment lasted 24 days and the minimum and maximum temperatures recorded were 20.6°C and 28.0°C respectively.

The CSIR creep testing apparatus is installed in a temperature controlled laboratory with the temperature maintained at 22°C.

Control specimens

Before performing the creep tests, uniaxial compression tests were conducted to determine strength as well as deformability characteristics for the material. This data was necessary in order to plan the stress levels for the creep cycles.

Number of creep stages

For the quartzite the total number of creep stages was 24. The reason for this was that the compressive strength had been underestimated due to the low strength of the control

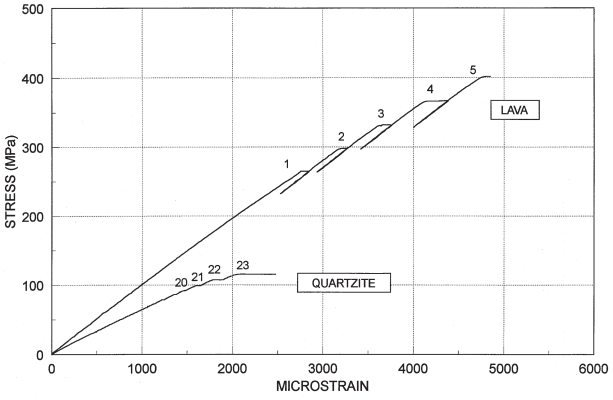

Figure 4—Stress-strain curves for quartzite and lava during the creep tests

specimen. It was subsequently established that the strength of the control specimen had been influenced by a pre-existing plane of weakness. This impacted on the stress level chosen for the first creep stage as well as on the magnitude of the subsequent load increments. Only the last four creep stages showed significant creep. Therefore the detailed evaluations described in the following sections were only done on these four creep stages.

For the lava the number of creep stages was 4.

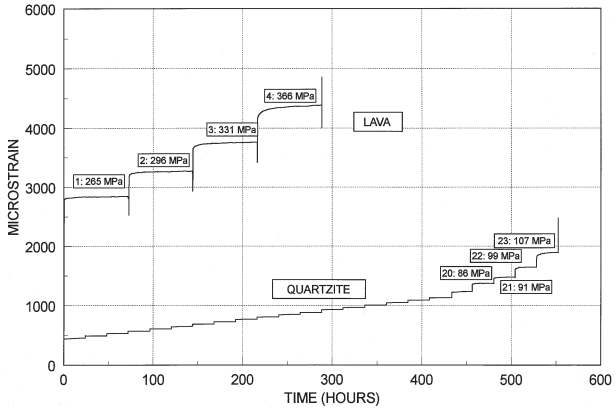

Figure 5—Complete strain vs time record for the quartzite and lava specimen during the creep tests

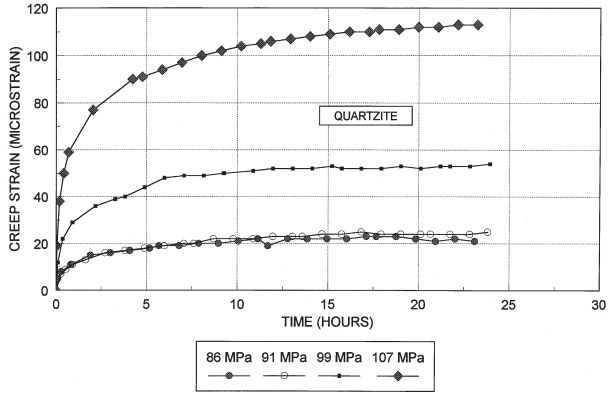

Figure 6a—Incremental creep curves at the different stages for quartzite

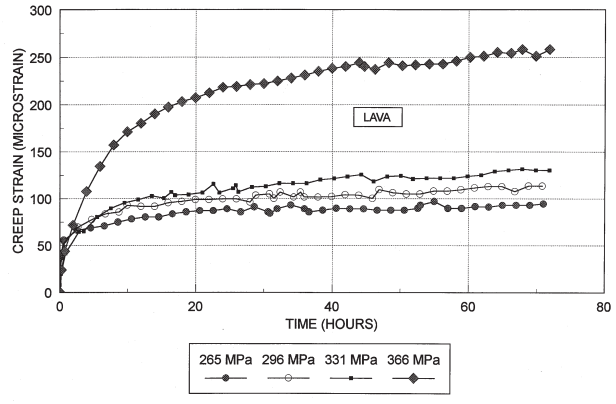

Figure 6b—Incremental creep curves at the different stages for lava

Results for laboratory specimens: Quartzite and Lava

The complete stress-strain curves are illustrated in Figure 4. Figure 5 shows the complete strain-time records while Figures 6a and 6b show the incremental creep strain as a function of time for the individual creep stages for the quartzite and the lava specimens respectively.

Effect of stress level on the secondary creep phase

It is well known for soft rocks that the creep rate of the secondary phase (steady-state creep rate) depends on the stress level[2]. From Figures 6a and 6b, this also appears to be true for the creep of lava and quartzite specimens. The most widely used steady-state creep law for salt is[3]

$$\dot{\varepsilon} = A\left(\sigma_1 \pm \sigma_3\right)^n e^{\pm\frac{Q}{RT}} \qquad [7]$$

where $\dot{\varepsilon}$ is the steady-state creep rate, A is a constant, σ_ι is a principal stress, Q is the activation energy for the creep mechanism, R is the universal gas constant and T is the temperature in degrees Kelvin. For both rock types, the tests were conducted at a constant temperature under uniaxial conditions. Equation 7 can therefore be reduced to

$$\dot{\varepsilon} = A'\sigma^n \qquad [8]$$

where

$$A' = Ae^{\pm\frac{Q}{RT}}$$

with units $Pa^{-n}s^{-1}$ and $\sigma = \sigma_1$ is the applied axial stress. The coefficient n can be determined from the slope of the curve of a $\log(\dot{\varepsilon})$ vs $\log(\sigma)$plot. Figure 7 show these graphs for typical lava and quartzite specimens. The linear nature of the curves illustrate the applicability of equation 8 as a model. The values of *n* are given in Table II.

Table II

Rock	Maximum strain x 10^{-3}	Maximum Stress MPa	Exponent *n*
Lava	4.1	329	3.5
Quartzite	1.9	107	9.1*
Granite (Lama and Vutukuri[2])	1.0	344.8	3.3
Shale (Lama and Vutukuri[2])	3.0	9.7	2.7

* See comment in text

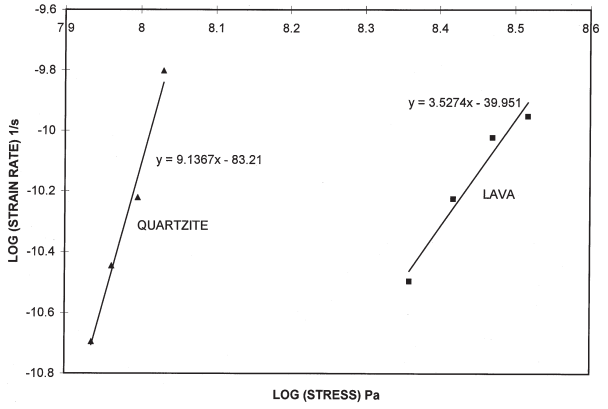

Figure 7—Log (strain rate) versus Log (stress) for lava and quartzite. The straight lines were fitted using linear regression

The value of n=3.5 for the lava specimen is of the same order as that obtained for the granite and shale. The value of n=9.1 for the quartzite is however much larger and needs to be confirmed by further experiments. It is possible that this value is too high as the time duration of individual loading steps for the quartzite was only 24 hours. Dusseault and Fordham[3] suggested that the steady-state creep rate can only be calculated after 4 to 5 days of measurements at a particular stress level. For the quartzite the strain-rate for the assumed secondary phase could still be artificially high due to the influence of primary creep.

Figure 8 illustrates a comparison between the strain rate of quartzite and that of lava in the secondary creep phase for different stress levels. The single datum point from Roux and Denkhaus[4] is also included. It is of significance that the quartzite samples experience strain rates which are comparable to lava at less than a third of the stress levels. Mining in quartzite host rock as opposed to lava at a particular depth will lead to a more stable fracture zone extending further away from the stope. At the boundary between fractured and unfractured rock, the intact rock will undergo secondary creep leading to the time-dependent formation of new fractures. This time-dependent process zone will extend further into the rock for quartzite. As stable fracturing dissipates energy, this behaviour may be advantageous in reducing violent outbursts. Mining of the Ventersdorp Contact Reef (lava hangingwall, quartzite footwall) in areas where the lava is particularly hard can be problematical due to the rolling nature of the reef. In areas where the reef rolls into the footwall, the mining is sometimes slow to follow, resulting in mining taking place entirely in the lava. The stable formation of the fracture zone could then be disrupted leading to face bursting. This phenomenon has been observed at mines in the Carletonville area (Handley[29]).

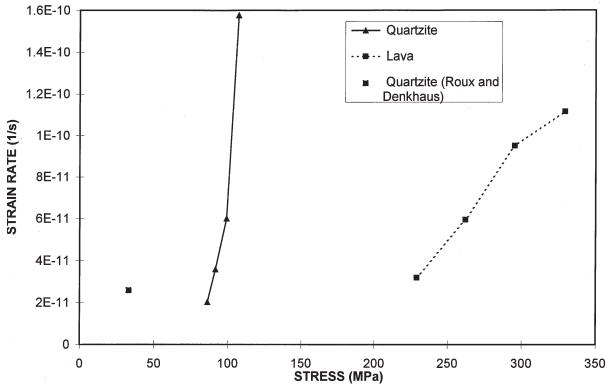

Figure 8—Strain rate of the secondary creep phase as a function of stress for lava and quartzite

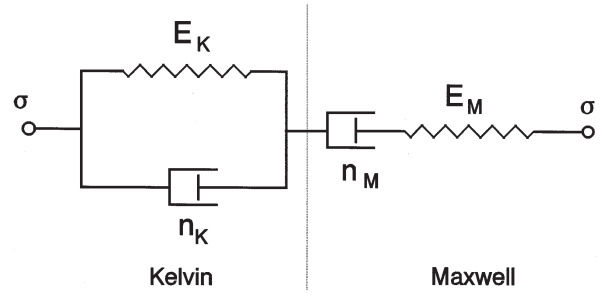

Figure 9—Burgers viscoelastic model

Rheological parameters for the laboratory creep of lava and quartzite

The viscoelastic rheological parameters for the laboratory specimens were calculated to facilitate comparison with underground measurements. The Burgers viscoelastic model (Figure 9) has been used frequently to model laboratory creep results as both the primary and secondary phase can be simulated. Lama and Vutukuri[2] derived the time-dependent strain for the Burgers model as

$$\varepsilon_t = \frac{\sigma}{E_M} + \frac{\sigma t}{3\eta_M} + \frac{\sigma}{E_K}\left(1 \pm e^{-\frac{E_K t}{3\eta_K}}\right) \qquad [9]$$

Table III

Source	E_M (GPa)	E_K (GPa)	η_M (GPa.h)	η_K (GPa.h)
Quartzite laboratory creep	60	1400	4.5×10^4	900
Lava laboratory creep	88	2100	1.8×10^5	3800
Deelkraal Goldmine *in situ* measurements	147	5000	2.3×10^3	250

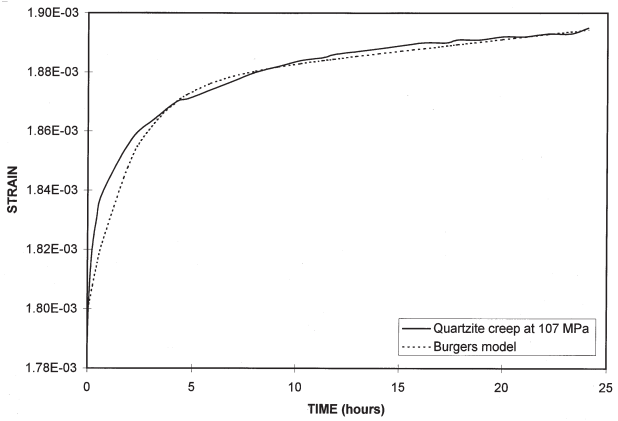

Figure 10a—Burgers viscoelastic model fitted to the creep of quartzite at a constant stress of 107 MPa

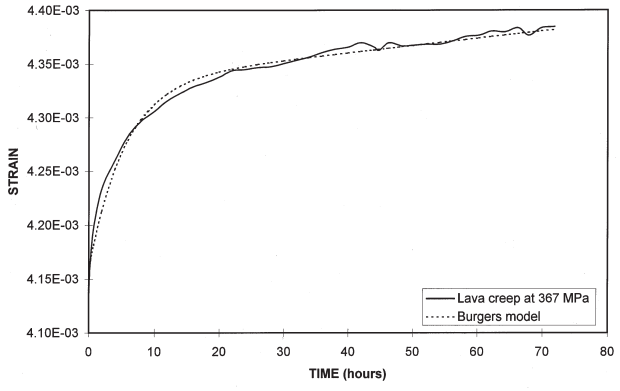

Figure 10b—Burgers viscoelastic model fitted to the creep of lava at a constant stress of 367 MPa

where E_M and E_K are the Young's moduli for the Maxwell and Kelvin units, η_K and η_M are the viscosity coefficients for the Kelvin and Maxwell units and t is time. This model was fitted to the data of the last creep stage for the quartzite and lava specimens. The results are illustrated in Figures 10a and 10b. The calibrated parameters are included in Table III for comparison with underground data. The strain rate of the secondary phase is determined by the viscosity coefficient η_M. The quartzite has a lower value of η_M at a much lower stress and will therefore be prone to higher creep rates in the secondary phase than the lava.

From the discussion in the previous section it follows that η_M is not a fundamental material constant but a function of stress and temperature, $\eta_M=f(\sigma,T)$. To describe this dependence, the following derived model utilises the empirical creep law just described. For the Maxwell model, the steady-state strain is given as[2]

$$\dot{\varepsilon} = \frac{\sigma}{3\eta_M} \cdot \qquad [10]$$

Inserting equation 7 and rearranging gives

$$\eta_M = \frac{\sigma_1}{3A\left(\sigma_1 \pm \sigma_3\right)^n e^{-\frac{Q}{RT}}} \cdot \qquad [11]$$

As the tests were conducted at a constant temperature under uniaxial conditions, equation 11 becomes

$$\eta_M = \frac{\sigma^{1\pm n}}{3A'} \qquad [12]$$

with $\sigma = \sigma_1$ the applied axial stress. This equation is plotted in Figure 11 using calibrated values of n and A´ together with the values of η_M obtained directly for the creep of the lava specimen at the different stress levels. The experimental results illustrate the clear stress dependence of the viscosity coefficient. Equation 12 gives a similar trend and appears to be successful in describing this stress dependancy.

Time-dependent behaviour of hard rock on a mining scale

To analyse continuous closure data, Malan[30] derived a Burgers viscoelastic convergence solution for a parallel-sided panel (Appendix A1). Care should, however, be exercised in the application of this model as it is not valid for stopes where total closure has taken place in the back area and where the geometry is such that the assumption of plain strain is impossible.

Closure data collected from a stope with 200 m span in Deelkraal Gold Mine suited these requirements. The Ventersdorp contact reef is mined with the hangingwall consisting of lava and the footwall of quartzite. The depth of the excavation was 2700m, the dip 25 degrees and the closure instrument was installed 16,6 m from the face. After the blast (one side only), the increase in span was 1,4 m. The Burgers convergence model was fitted to the data as illustrated in Figure 12. The calibrated values for the model are given in Table III and compared with values obtained for the laboratory creep of quartzite and lava specimens.

For the Burgers model, the instantaneous response after load application or change is determined by the Maxwell modulus E_M. From Table III this value, calibrated for the underground measurements, is relatively large at 147 MPa indicating that the instantaneous closure at the time of face advance is quite small. This is in agreement with McGarr[18] who provided data and an analysis illustrating that the instantaneous closure at blasting time is small. This effect is caused by the fractured nature of the face ahead of the stope. The stress carried by this fractured rock ahead of the face is less than would be expected for a stope where no fracturing took place. Blasting in this fracture zone results in instantaneous redistribution of stress. This stress distribution is, however, smaller than expected for a completely elastic material. When simulating this process with viscoelastic theory (which cannot model failure), the calibrated value of E_M will appear large because of the smaller instantaneous closure behaviour.

The behaviour of the rock in the secondary phase of creep is described by the Maxwell viscosity η_M. It is clear from the table that this value for the *in situ* measurements is more than an order of magnitude smaller for the quartzite specimen and two orders smaller than the lava specimen. Similarly, Kranz and Estey[31] found that the viscosity values calculated in a deep hard rock mine are two orders smaller than those for unfractured granite slabs. There must therefore be another mechanism dominating the time-dependent behaviour of the rockmass surrounding stopes.

Following the work of Hodgson[15] and Adams and Jager[17] described above, the rheological properties of the fracture zone, and particularly time-dependent fracture formation, must play a prominent role in the underground time-dependent behaviour. This is in agreement with other workers (Tan and Kang[32]; Schwartz and Kolluru[33]). Realistic modelling of the time-dependent rock behaviour therefore needs to simulate the rheological behaviour of discontinuities and the interaction between these discontinuities. To address this problem, Napier and Malan[34] developed a time-stepping solution scheme to solve multiple viscous discontinuities in a boundary element code. This framework was used by Malan and Spottiswoode[35] to implement a viscoplastic displacement discontinuity interface model with time-dependent strength properties. This model (Appendix A2) is used in the next section to simulate the time-dependent fracture processes surrounding a deep stope.

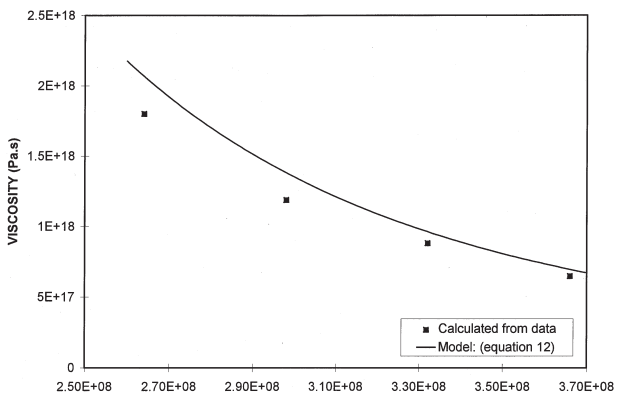

Figure 11—Dependence of the viscosity coefficient η_M on the applied stress magnitude

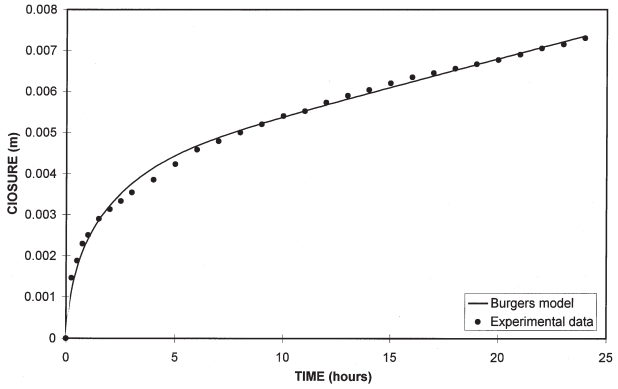

Figure 12—The Burgers convergence model fitted to underground measurements

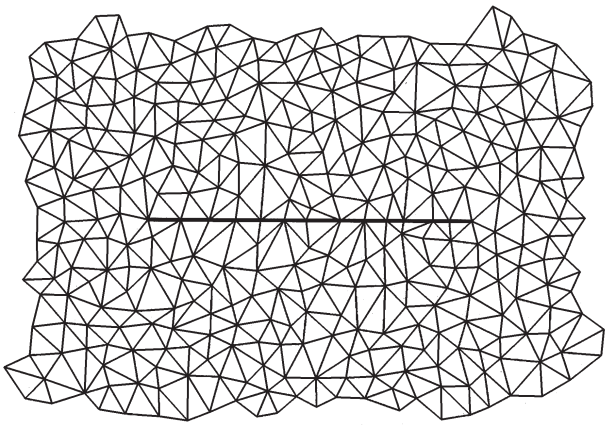

Figure 13—Initial random distribution of potential fracture planes surrounding the reef

Incremental mining of a tabular stope: Numerical results

Stope modelling was undertaken by covering the problem space by a random mesh of viscoplastic discontinuities. Figure 13 shows a typical distribution used. This distribution should be considered as potential fracture surfaces as they are initially intact with a prescribed strength determined by the failure criteria of the model. Mining was undertaken in an incremental fashion allowing the progressive evolution of the fracture zone. Due to computer memory limitations, the number of elements is limited. The object of this modelling should therefore be seen as studying the effect of the time-dependent fracture process and not to replicate observed fracture patterns.

Figure 14 illustrates the typical development of the fracture zone following a series of mining steps. The discontinuities shown are all those mobilised up to that particular point in time. Due to the low density of the initial tessellation, this fracture pattern is at best only a coarse approximation of that observed underground. This is especially notable in the immediate area of the stope faces where the density of fracturing is much lower than expected for underground stopes. The model has nevertheless proved to be useful for simulating the time-dependent processes in the rock. An important consequence of the prescribed viscoplastic behaviour is that the additional fracturing caused by a sudden increase in stress occurs in a time-dependent fashion. After a mining increment, the existing discontinuities surrounding the stope are subjected to an increase in mining- induced stress. Those discontinuities subjected to stresses above the yield surface relax in a time-dependent manner according to the constitutive model. This relaxation process causes a stress transfer to the solid rock at the edge of the fracture zone. New fractures then form in these positions as a time-dependent process. For the example given, the increase in cumulative fracture length as a function of time after a blast is illustrated in Figure 15. It should be emphasised that there are no changes in the excavation dimension during this time period. Similarly to Adams and Jager's[17] observations, the majority of new fractures formed within a short period after the blast, and the rate of fracturing then diminished until the next blast. A comparison between this numerical time-dependent fracture process and cumulative seismicity after blasting can be found in Malan and Spottiswoode[35]. A good fit was obtained illustrating the applicability of the model.

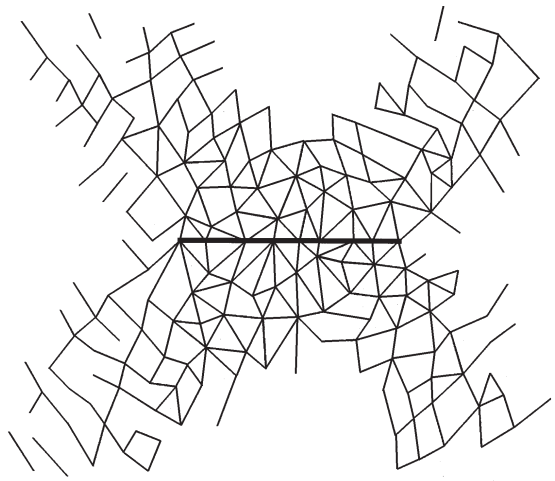

Figure 14—Development of the fracture zone 24 hours after the 9th mining increment. The stope is represented by the thick black line

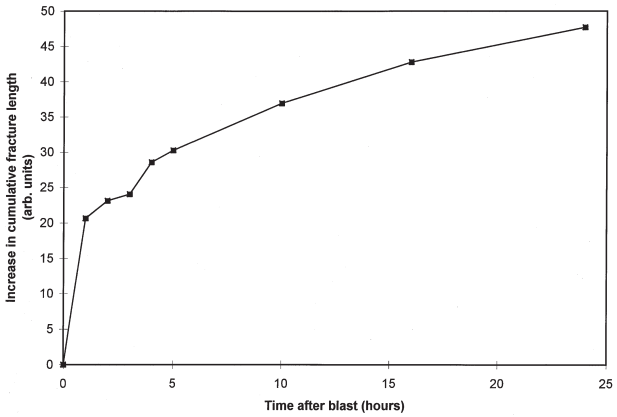

Figure 15—Increase in cumulative fracture length after the 9th mining increment

The time-dependent fracture process leads to the typical stope closure profile illustrated in Figure 16. As expected the highest rate of closure occurs after blasting time and this decays until the next blast takes place. When comparing this with underground observations (e.g. Figure 12, and Leeman[14]) it is clear that similar closure trends are predicted by the model.

As mentioned in the introduction, McGarr[18] investigated the stope closure rate throughout the week at East Rand Proprietary Mines (Figure 17). The closure is given during six-hour intervals with the value at the middle of a given six-hour period plotted in the Figure 17. The experimental data have been averaged over 30 weeks. Results obtained from numerical modelling illustrates similar trends. The model parameters used are μ' = le-8 MPa^{-1}s^{-1}m, S_p = 20MPa, S_r = 0 MPa, α = 0.005 s^{-1}, β = 0.005 s^{-1}, φ_p = 30, φ_r = 20 (See Appendix A2). The highest rate of closure occurs during the six-hour interval that includes the times of face advance. The rate also increases throughout the week until Sunday when no blasting takes place and the rock is allowed to relax further. There is however a weak fit between the experimental data and numerical results for the periods of decreasing rate of closure after the blast. This is caused by the low density of fracturing ahead of the faces in the numerical model. Mining in this unfractured stressed rock results in relatively higher increase in convergence for the period which includes the blast. The peak values of the modelling results also show some erratic behaviour because of the discontinuous nature of the model. As the density of fractures in the tessellation is low, the rate of convergence is still strongly influenced by the measurement position and the orientation of the new fractures activated by each mining step. If fractures with a favourable orientation are activated in a particular step, higher rates of convergence are suddenly experienced. That this erratic behaviour almost follows the same trend as the peak values of the underground measurements is purely accidental. Other tessellation patterns and measurement positions will give different peak values for each step. Work is currently undertaken to increase the number of potential fracture planes in the tessellation to alleviate this problem.

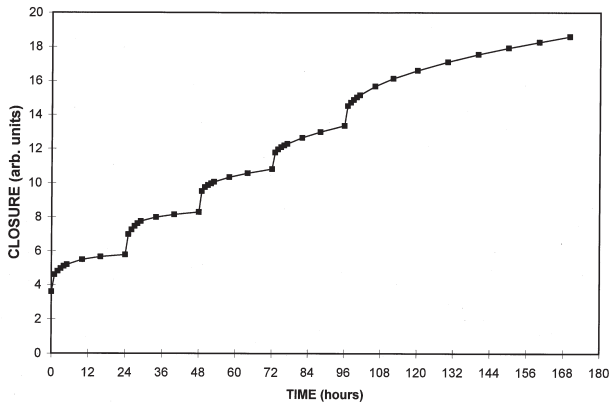

Figure 16—Numerical stope closure as a function of time. Blasting took place at 0, 24, 48, 72 and 96 hours

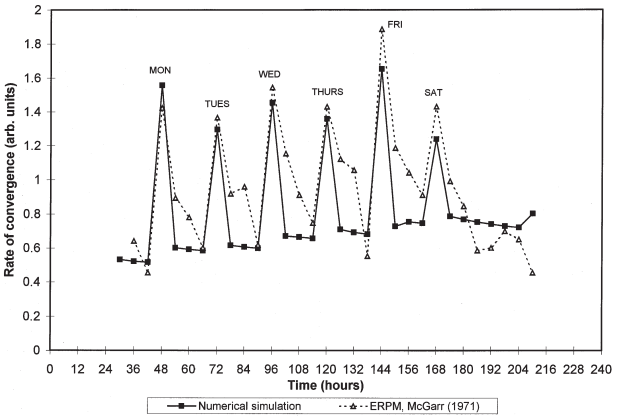

Figure 17—Numerical and experimental rate of closure as a function of time. The experimental data are from East Rand Proprietary Mines (after McGarr[18], see text)

Conclusions

In deep level hard rock mining, the rheological behaviour of the rock is important as time-dependent aseismic processes can lead to a stable dissipation of energy reducing violent outbursts. Underground closure measurements, observations of time-dependent fracture formation and seismic data indicate that the rock in deep South African gold mines shows notable time-dependent behaviour. The objective of this work was to quantify the time-dependent rock behaviour for laboratory specimens and underground conditions.

Laboratory creep experiments of quartzite and lava specimens indicate that these rocks undergo measurable creep strain at stress values below the failure strength. The creep curves illustrate the typical primary and secondary behaviour. The strain rate in the secondary creep phase is strongly dependent on the stress level for both rock types. This dependence can be successfully modelled with a stress power law. The quartzite specimens are however prone to more significant creep than the lava samples. For the type of quartzite and lava tested, comparable creep rates are obtained if the stress in the quartzite is approximately one-third of that in lava.

The time-dependent rock behaviour observed for deep level stopes is much more significant than what can be expected of the creep of intact rock. A Burgers viscoelastic model fitted to the creep of intact laboratory specimens and *in situ* closure measurements, indicates viscosity values two orders smaller for rock on a mining scale. Observations and numerical modelling indicate that underground behaviour is governed mainly by rheological behaviour of the fracture zone and the resulting time-dependent formation of new fractures. After a blast, the existing fractures surrounding the stope are subjected to an increase in mining induced stress. The fracture zone relaxes in a time-dependent fashion transferring stress to the more solid rock. New fractures then form in these positions as a time-dependent process. The majority of the fractures however form within a short period of the blast. Numerical modelling showed that this process can be simulated by a large assembly of discontinuities each behaving in a viscoplastic fashion. Of significance, is that the continuous closure profiles observed can be simulated and

therefore explained by this delayed fracture model.

Almost no experimental data on the time-dependent behaviour of fractures and other discontinuities subjected to shear is available however. Therefore, this study is currently directed towards a laboratory investigation to determine the applicability of the time-dependent constitutive model and parameters for discontinuities. Further comparison with underground observations and closure measurements is also required.

Acknowledgements

This work forms part of the rockmass behaviour research programme of Rock Engineering, CSIR Division of Mining Technology. The authors acknowledge the financial assistance and support received from the Safety in Mines Research Advisory Committee (SIMRAC). D.F. Malan is working towards a Ph.D. degree at the University of the Witwatersrand and the work described here also forms part of that study. The authors would like to thank Dr J.A.L. Napier, Dr M.F. Handley and an anonymous referee for reviewing the manuscript and making several useful comments.

Appendix

A1: Burgers viscoelastic convergence solution for a tabular parallel-sided panel in isotropic ground

If it is assumed that the rock behaves elastically in hydrostatic compression and as a Burgers model (see Figure 9) in distortion, Malan[30] showed that the incremental viscoelastic convergence $\Delta S_z(x,t)$ for a stope with face advance of $\Delta 1$ at one side only can be written as

$$\Delta S_z(x,t) = \pm 4 W_z \left(1 + \frac{dx}{2}\right) F(t) \left[\sqrt{\left(L + \frac{\Delta 1}{2}\right)^2 \pm \left(x \pm \frac{\Delta 1}{2}\right)^2} \pm \sqrt{L^2 \pm x^2}\right] \quad [A1]$$

where

$$F(t) = g_1 \left[1 + c_5 t + c_6 e^{\pm ft} + \left(c_7 \sinh\ \mathrm{bt} + c_8 \cosh\ \mathrm{bt}\right) e^{\frac{-ht}{2}}\right] \quad [A2]$$

and

$$b = \sqrt{\frac{\left(6Kp_1 + q_1\right)^2 \pm 24K\left(6Kp_2 + q_2\right)}{4\left(6Kp_2 + q_2\right)^2}} \quad [A3]$$

$$g_1 = \frac{2Kp_1q_1 + q_1^{\,2} \pm 2Kq_2}{4Kq_1^{\,2}} \quad [A4]$$

$$c_5 = \frac{2Kq_1}{2Kp_1q_1 + q_1^{\,2} \pm 2Kq_2} \quad [A5]$$

$$c_6 = \frac{2K\left(p_2q_1^{\,2} \pm p_1q_1q_2 + q_2^{\,2}\right)}{q_2\left(2Kp_1q_1 + q_1^{\,2} \pm 2Kq_2\right)} \quad [A6]$$

$$c_7 = \frac{q_1^{\,2}\left(\pm 12Kp_2q_1 + 6Kp_1q_2 \pm q_1q_2\right)}{2b\left(6Kp_2 + q_2\right)^2\left(2Kp_1q_1 + q_1^{\,2} \pm 2Kq_2\right)} \quad [A7]$$

$$c_8 = \frac{q_1^{\,2}q_2}{\left(6Kp_2 + q_2\right)\left(\pm 2Kp_1q_1 - q_1^{\,2} + 2Kq_2\right)} \quad [A8]$$

$$f = \frac{q_1}{q_2} \quad [A9]$$

$$h = \frac{Kp_1 + q_1}{6Kp_2 + q_2} \quad [A10]$$

and

$$p_1 = \frac{(1+v)\left(\eta_K E_M + \eta_M E_K + \eta_M E_M\right)}{E_K E_M} \quad [A11]$$

$$p_2 = \frac{\eta_K \eta_M (1+v)^2}{E_M E_K} \quad [A12]$$

$$q_1 = \eta_M \quad [A13]$$

$$q_2 = \frac{\eta_M \eta_K (1+v)}{E_K} \quad [A14]$$

$$W_z = \frac{\pm \gamma \mathrm{H}}{2}\left[(1+k) + (1 \pm k)\cos 2\alpha\right] \quad [A15]$$

$$d = \frac{\sin\alpha \cos\beta}{H} \quad [A16]$$

L = half span of the stope
x = distance from the centre of the stope (origin of co-ordinate system)
γ = specific weight of the rock
H = depth below surface
k = ratio of horizontal to vertical stress
α = dip of the reef
β = angle between x-axis and the dip
K = bulk modulus

The z-axis is perpendicular to the plane of the excavation and points towards the footwall. The two-dimensional section is taken parallel to a plane normal to the y-axis (See Figure A1). This model is however only applicable to stopes without total closure in the back area and where the geometry is such that the assumption of plain strain is possible.

A2: Formulation of a viscoplastic displacement discontinuity model

Figure A2 illustrates a discontinuity with the shear component D_s and normal component D_n. Malan and Spottiswoode[35] showed that if the discontinuity behaves in a viscoplastic fashion (Perzyna[36]) the incremental increase in discontinuity components for a small timestep Δt, can be

given as

$$\Delta D_s = \mu' l \langle F \rangle \Delta t$$
$$\Delta D_n = | \Delta D_s | \tan\Psi \quad [A17]$$

where ψ is the dilation angle, μ' is the discontinuity fluidity constant with units $Pa^{-1}s^{-1}m$ and l assumes the value -1 or +1 depending on the direction of the shear stress. $\langle F \rangle$ is the yield function and assumes a value of 0 if the stresses are below the shear strength of the discontinuity.

When assuming a Mohr-Coulomb model, F can be given by

$$F = | \tau | - S_c + \sigma_n \tan \phi_c \quad [A18]$$

where τ is the shear stress and S_c and ϕ_c are the current values of cohesion and friction angle respectively. The mobilised discontinuities can undergo a time-dependent reduction in strength (Malan and Spottiswoode[35]) according to

$$S_c = S_r + \left(S_p \pm S_r\right) e^{-\alpha t} \quad [A19]$$

$$\phi_c = \phi_r + \left(\phi_p - \phi_r\right) e^{-\beta t} \quad [A20]$$

where α is the cohesion decay factor, β is the friction decay factor and S_r and ϕ_r the residual values of cohesion and friction angle. The time t is that accumulated for each discontinuity which is loaded to within 80% or above of the shear strength.

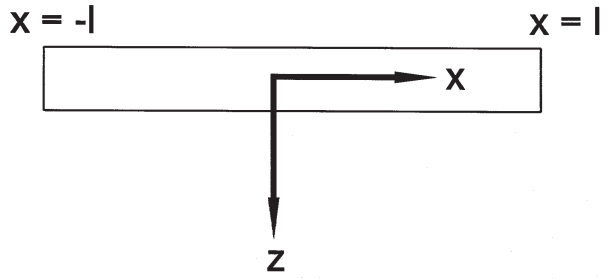

Figure A1—Co-ordinate system used for the Burgers convergence model

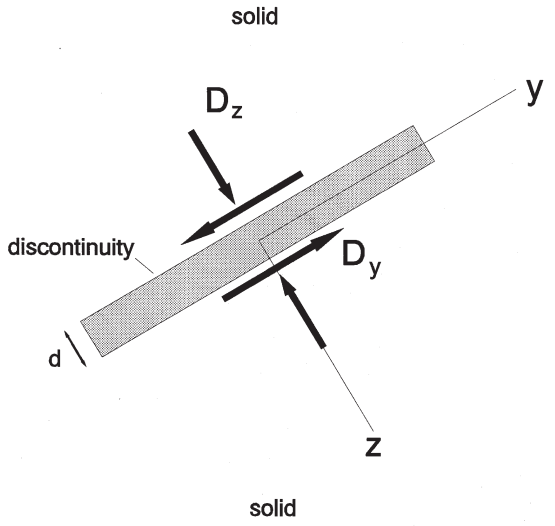

Figure A2—Components of the displacement discontinuity vector

References

1. Griggs, D. Creep of rocks. *J. Geol.* vol. 47, 1939. pp. 225–251.
2. Lama, R.D. and Vutukuri, V.S. Handbook on mechanical properties of rocks—Testing techniques and results. Volume III. *Trans Tech Publications,* Germany, 1978. pp. 209–320.
3. Dusseault, M.B. and Fordham, C.J. Time-dependent behavior of rocks. *Comprehensive rock engineering*, vol. 3, Hudson, J.A. (ed.). Pergamon Press, 1993, pp. 119–149.
4. Roux, A.J.A. and Denkhaus, H.G. An investigation into the the problem of rock bursts- An operational research project. *J. Chem. Metall. Min. Soc. S. Afr.,* vol. 55, 1954. pp. 103–124.
5. Denkhaus, H.G., Hill, F.G., and Roux, A.J.A. A review of recent research into rockbursts and strata movement in deep-level mining in South Africa. Ass. *Min. Mngrs. S. Afr.*, 1958. pp. 245–268.
6. Pomeroy, C.D. Creep in coal at room temperature. *Nature*. vol. 178, 1956. pp. 279–280.
7. Potts, E.L.J. and Hedly, D.G.F. The influence of time-dependent effects on the design of mine pillars. *Int. Bureau of Rock Mech. Proc. 6th Int. Conf.* Leipzig, 1964.
8. Wiid, B.L. The time-dependent behaviour of rock: Considerations with regard to a research programme. CSIR *Report* MEG 514, 1966.
9. Kovács, I.K.A. An investigation of the time-dependent behaviour of solid rock in uniaxial compression. CSIR *Report* MEG 1032, 1971.
10. Rock Mechanics Research Group, National Mechanical Engineering Institute, CSIR. Report on the non-elastic properties of rock from borehole number 3034 from Hartebeestfontein gold mine. CSIR *Report* MEG 563, 1963.
11. Bieniawski, Z.T. Mechanism of brittle fracture of rock–Part III–Fracture in tension and under long term loading. *Int. J. Rock Mech. Min. Sci.,* vol. 4, 1967. pp. 425–430.
12. King, R.G., Jager, A.J., Roberts, M.K.C., and Turner, P.A. Rock mechanics aspects of stoping without back-area support. COMRO (Now CSIR Miningtek) *Research Report* no. 17/89. 1989.
13. Gürtunca, R.G. Results of a classified tailings monitoring programme at Vaal Reefs. COMRO (Now CSIR Miningtek) *Internal Report* no. 614. 1989.
14. Leeman, E.R. Some measurements of closure and ride in a stope of the East Rand Proprietary Mines. *Pap. Ass. Min. Mngrs. S.Afr.* vol. 1958–1959, 1958. pp. 385–404.
15. Hodgson, K. The behaviour of the failed zone ahead of a face, as indicated by continuous seismic and convergence measurements, *C.O.M. Res. Rep.* 31/61, Transvaal and Orange Free State Chamber of Mines Res. Org. 1967.
16. Cook, N.G.W., Hoek, E., Pretorius, J.P.G., Ortlepp, W.D. and Salamon, M.D.G. Rock Mechanics applied to the study of rockbursts. *J. S. Afr. Inst. Min. Metall.* vol. 66, 1966. pp. 435–528.
17. Adams, G.R. and Jager, A.J. Petroscopic observations of rock fracturing ahead of stope faces in deep-level gold mines. *J. S. Afr. Inst. Min. Metall.*, vol. 44, 1980. pp. 204–209.
18. McGarr, A. Stable deformation near deep-level tabular excavations *J. Geophys. Res.* vol. 76, no 29, 1971, pp. 7088–7106.
19. Malan, D.F. A viscoelastic approach to the modelling of the transient closure behaviour of tabular excavations after blasting. *J. S. Afr. Inst. Min. Metall.,* vol. 95, 1995. pp. 211–220.
20. Cook, N.G.W. Seismicity associated with mining. *Eng. Geol.* vol. 10, 1976. pp. 99–122.
21. McGarr, A. Dependence of magnitude statistics on strain rate. *Bull. Seism. Soc. Am.*, vol. 66, no. 1, 1976. pp. 33–44.
22. Stewart, R.D. and Spottiswoode, S.M. A technique for determining the seismic risk in deep-level mining. *Rockbursts and Seismicity in Mines*. R. P. Young, (Ed.). 1993. pp.123–128.

23. VAN ASWEGEN G. and BUTLER A.G. Applications of quantitative seismology in South African gold mines. *Rockbursts and Seismicity in Mines,* R.P. Young (ed.). Balkema, 1993. pp. 261–266.
24. MENDECKI, A.J. Management strategies and rockburst prediction. *Proc. SIMRAC/SAIMM Symposium,* Johannesburg, 1996.
25. MENDECKI, A.J. Real time quantitative seimology in mines. Keynote lecture. *Rockbursts and Seismicity in Mines*, R.P. Young (ed.). Balkema, 1993. pp. 287–295.
26. VOGLER, U.W. Creep tests on argillaceous footwall quartzite. CSIR *Report* EMA-C 9052. 1990.
27. VOGLER, U.W. and DRESCHER, K. Creep tests on Ventersdorp Lava. CSIR Internal Report. In preparation. 1996.
28. TAN, T-K. The importance of creep and time-dependent dilatancy, as revealed from case records in China. Rock testing and site characterisation. *Comprehensive Rock Engineering,* vol. 3, J.A. Hudson (ed.). 1993. pp. 709–744
29. HANDLEY, M.F. Personal communication, 1996.
30. MALAN, D.F. Discussion of reference 19. A viscoelastic approach to the modelling of transient closure behaviour of tabular excavations after blasting. *J. S. Afr. Inst. Min. Metall.*, vol. 96, 1996. pp. 159–164.
31. KRANZ, R.L. and ESTEY, L.H. Listening to a mine relax for over a year at 10 to 1000 meter scale. *Proc. 2nd North Am. Rock Mech. Symp:* NARMS '96, M. Aubertin, F. Hassani and H. Mitri, (eds.). Montreal, Jun. 1996. pp. 491–498.
32. TAN, T-K. and KANG, W. Locked in stresses, creep and dilatancy of rocks, and constitutive equations. *Rock Mechanics,* vol. 13, 1980. pp. 5–22.
33. SCHWARTZ, C.W. and KOLLURU, S. The influence of stress level on the creep of unfilled rock joints. *Proc. 25th Symp. Rock Mech.* 1984. pp. 333–340.
34. NAPIER, J.A.L. and MALAN D.F. Viscoplastic modelling of rock deformation using an explicit displacement discontinuity formulation. Submitted to *Int. J. Rock Mech. Min. Sci. & Geom. Abstr.*, 1996.
35. MALAN, D.F. and SPOTTISWOODE, S.M. Time-dependent fracture zone behaviour and seismicity surrounding deep level stoping operations. Accepted for publication in P*roc. 4th Int. Symp. Rockbursts & Seismicity in Mines*, S.J. Gibowitz (eds.). Krakow, Poland, Aug. 1997.
36. PERZYNA, P. Fundamental problems in viscoplasticity. *Adv. Appl. Mech.,* vol 9, 1966. pp. 243–377. ◆

New software ensures safer mine environment*

New software that will assist mining engineers in the design of safer underground workings has recently been developed by the Department of Mining Engineering at the University of Pretoria. A workshop was held to announce the computer program, known as JBlock. The program evaluates the potential for rock falls in blocky rock often encountered in mining excavations. The program calculates the effect of different types and layouts of support on potential rock falls. This enables engineers to optimise the layout of support for their local rock conditions.

Rock falls are a major cause of accidents in underground mines. The falls are often caused by natural planes of weakness in the rock being mined. In deep mines, stress fractures may also exist in the rock, further increasing the hazard of rock falls. Rock engineers require a design method to realistically model the types of rock block which are formed by the intersection of these natural and stress-induced planes of weakness. They also need a method to determine how the supports installed in the workings will interact with the rock blocks. This need is addressed by the program JBlock.

JBlock was developed by Mr Essie Esterhuizen of the Department of Mining Engineering. The development was initially supported by Samancor. The program is now commercially available and has aroused much interest in the rock engineering fraternity. The workshop was attended by 40 persons from different South African mining groups. ◆

Representatives from the mining industry who attended the launch. Mr Essie Esterhuizen is on the extreme left

** Issued by: Mr G.S. Esterhuizen, Dept. of Mining Engineering, University of Pretoria.*

Revamped SAIEE bursary scheme offers more than financial help*

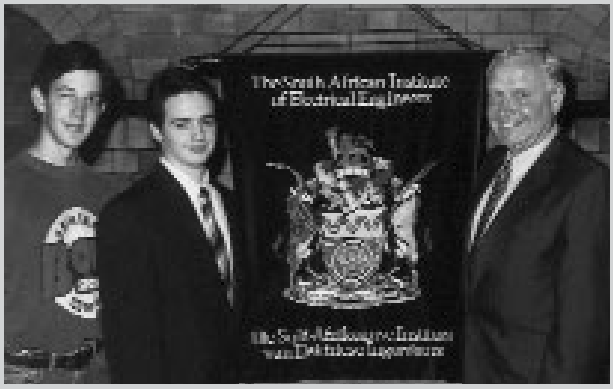

Twenty-three bursaries, valued at R161 000.00, have been awarded by the South African Institute of Electrical Engineers (SAIEE) this year. This three-fold increase of funds previously set aside for bursaries has been structured to meet future demand for electrical engineers and technicians. The SAIEE's Hermann Broschk (right), responsible for the Institute's bursary loan scheme and a member of its education and training committee, says several innovative strategies were recently adopted. Among these are that the Institute will administer bursaries for companies without facilities to do so themselves, and will also administer bursaries to which small companies can collectively contribute and which will bear the names of the contributing companies as sponsors. With Broschk are HT Aspinall bursars Hans Zacher of the University of the Witwatersrand (left) and Daniel van Niekerk of Wits Technikon. The HT Aspinall Bursary Fund is administered by the SAIEE and gives preference to Technikon Witwatersrand and University of the Witwatersrand students. ◆

** Issued by: Lynne Hancock Communications, P.O. Box 180 Witkoppen,* 2068.

Matla awards R1,7-million dust suppression contract to CDC*

Colliery Dust Control (CDC) of Springs has secured a major coal dust suppression systems contract with Matla Colliery.

The R1,7-million contract is for provision of dust suppression equipment for 12 continuous miners—representing about 75% of the machines deployed in the mine's three shafts.

The contract involves manufacture and supply of scrubber boxes, water-powered air movers and spray fan systems operating together as an integrated system on each of the continuous miners.

Matla Colliery, near Kriel in Mpumalanga, is one of Ingwe Coal Corporation's collieries. The order is the first major order by an Ingwe group colliery for CDC equipment.

Prior to the order being placed CDC made available three scrubber boxes to Matla Colliery to use on their continuous miners to assist them in assessing their requirements.

CDC's range of dust suppression equipment for continuous miners is backed by a 24-hours-a-day spares and service operation and service exchange units, enabling mines to reduce their stockholding of key components without adversely affecting machine availability.

The CDC scrubber box is the most important component in the three-in-one integrated system which the company provides. A major feature of the scrubber box is its small-frame water-cooled motor which assures the reliability of the unit and virtually eliminates the risk of motor failure due to low inertia and minimal thermal cycling. ◆

** Issued by: J. Kraft Public Relations, P.O. Box 28552, Kensington 2101.*